Journal of Nuclear Materials 390–391 (2009) 246–249

Contents lists available at ScienceDirect

Journal of Nuclear Materials

journal homepage: www.elsevier.com/locate/jnucmat

Radiating divertor experiments in the HL-2A tokamak

L.W. Yan *, W.Y. Hong, J. Cheng, M.X. Wang, J. Qian, Y.D. Pan, Y. Zhou, W. Li, D.L. Yu, K.J. Zhao, Z. Cao, Q.W. Yang, X.R. Duan, Y. Liu

Southwestern Institute of Physics, Division 102, P.O. Box 432, Chengdu, Sichuan 610041, China

A R T I C L E   I N F O

PACS:
52.55.Rk
52.40.Db
52.25.Ya
52.40.Hf

A B S T R A C T

Radiating divertor experiments have been performed in HL-2A using different fueling methods, such as direct gas puffing (GP), supersonic molecular beam injection (SMBI), and noble gas injection in divertor. The plasma temperatures at inner and outer target plates can be decreased below 2 eV in completely detached plasma (CDP). Electron pressures at target plates, radiation power in divertor and the compression ratio (R_{p0}) of neutral gas pressures between the divertor and main chamber gradually drop during the detachment. Partial detachment first appears at inner target plate even if plasma density is very low. No clear high-recycling regime is observed before the detachment. It is more difficult to observe the partial detachment if the drift direction of magnetic field gradient is away from X-point because the electron temperature at inner target plate is higher than that at outer one.

1. Introduction

External impurity injection is considered necessary to decrease the divertor heat load in ITER to an acceptable level [1]. Radiating divertor experiments for meeting ITER requirements have been demonstrated in some large tokamaks, such as JT-60U [2], JET [3], DIII-D [4], and ASDEX-Upgrade [5]. Recently, they are also performed in HL-2A with different fueling methods. In addition, the divertor plasma parameters in HL-2A are simulated with the SOLPS5.0 code [6]. The results indicate that the neutral particle recycling is rather effective to impact divertor plasma parameters and neutral momentum loss appears even if the discharge density is very low. This effectiveness results in higher radial expansion of plasma pressure, particle and incident power fluxes in the divertor. The local 2-point model scaling in divertor physics is not obtained [7]. No clear high-recycling regime is observed before plasma detachment. These results have been confirmed by experiments.

2. Diagnostics arrangement

Contrasted with conventional open divertor, HL-2A tokamak has two rather closed divertor chambers [8], whose independent parameters of divertor plasma provide better benchmark for divertor physics. Many diagnostics have been developed for the benchmark. The plasma parameters in lower divertor are measured by 2 fixed flush probe arrays on inner and outer target plates [9], a movable probe array, a fast neutral pressure gauge (FG), a bolometer array, an infrared (IR) camera, a microwave interferometer, the visible lights such as D_α as well as CIII emission, and so on, as shown in Fig. 1. The edge parameters in main plasma are diagnosed by fast reciprocating probes, two movable probes, an FG, 3 bolometer arrays, a VUV spectrometer, a microwave reflectometer, visible lights, and so on. Electron density is measured by 8 channel HCN interferometer, while electron temperature is provided by Thomson scattering and ECE systems.

3. Experiment results

Radiating divertor experiments in HL-2A are conducted with lower single null configuration and deuterium discharges by different fueling methods, such as direct GP, SMBI at midplane, and noble gas injection in divertor. Typical discharge parameters are R = 1.65 m, a = 0.38 m, Bt = 1.4 T, I_p = 180 kA, q_a = 3.6, line-averaged density $n_e = (2–6) \times 10^{19}\ m^{-3}$, Greenwald density limit $n_G = 4.0 \times 10^{19}\ m^{-3}$. Normally, the Grad-B drift direction is toward X-point except where specified.

Fig. 2 shows a partially detached discharge obtained by strong GP at midplane. Here partial detachment means one target plate to be detached, while the CDP is two plates to be detached. Typically radiating power fraction in main plasma is 20–50% and D_α emission in divertor remains almost invariant in Fig. 2. The electron temperature and pressure at inner target drop after t > 150 ms even if plasma density is very low, indicating that the partially detached plasma first appears at inner target. The result is in agreement with the simulation one [6]. Electron temperatures and pressures at target plates gradually drop during the detachment, while the radiation power in main chamber and the com-

* Corresponding author.
E-mail address: lwyan@swip.ac.cn (L.W. Yan).

0022-3115/$ - see front matter © 2009 Elsevier B.V. All rights reserved.
doi:10.1016/j.jnucmat.2009.01.075

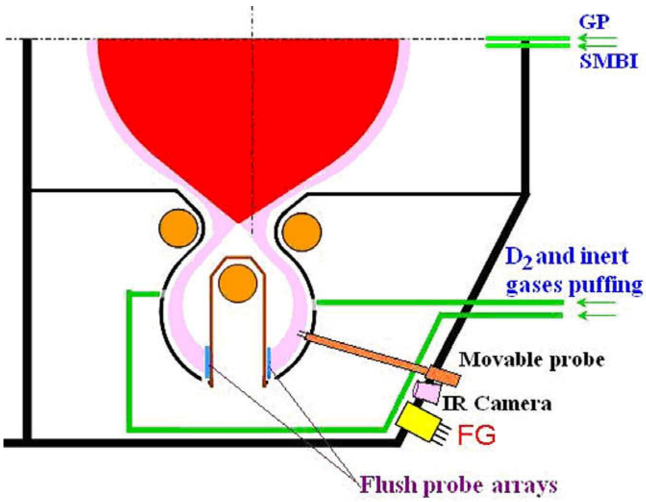

Fig. 1. The schematics of main divertor diagnostics and fuelling systems. The direct GP and SMBI are fuelled at midplane, while the divertor is fuelled with deuterium and noble gases. Seven sets of triple flush probes give electron temperature and density profiles at inner and outer divertor targets with spatial resolution of 1 cm. Two fast ionization gauges measure neutral particle pressures in main chamber and divertor. Movable probes can measure electron temperature and density profiles in divertor through shot by shot. An IR camera observes the surface temperature at outer target.

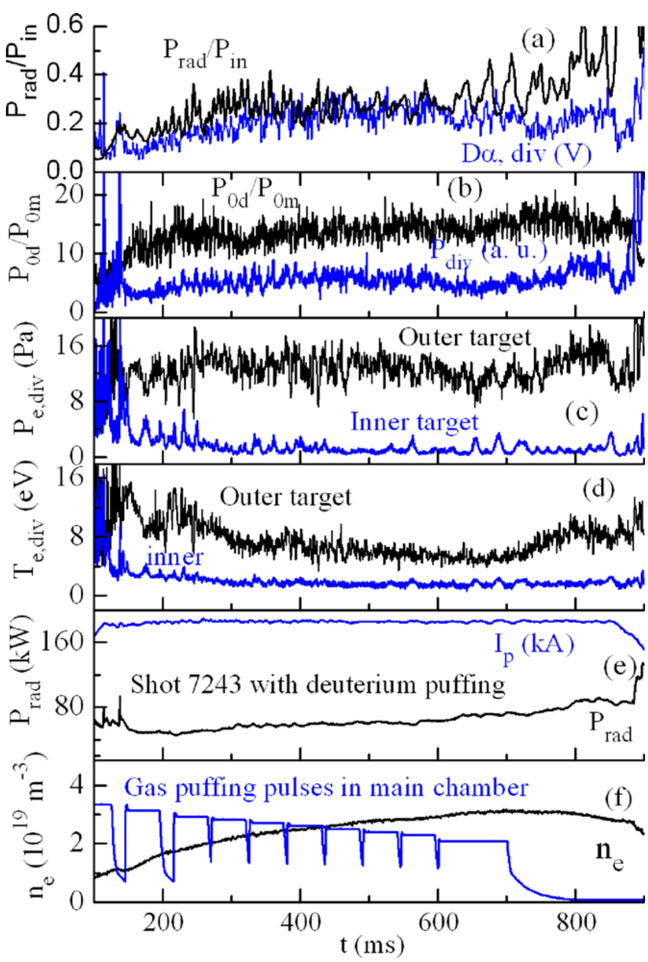

Fig. 2. Partially detached plasma obtained by strong GP at midplane. The curves are (a) the radiating power fraction in main plasma (P_{rad}/P_{in}) and the D_α emission in divertor, (b) the compression ratio ($R_{p0} = P_{0d}/P_{0m}$) of neutral particle pressures between divertor and main chamber, radiation power in divertor (P_{div}), (c) electron pressures at inner and outer targets, (d) electron temperatures at inner and outer targets, (e) radiation power in main plasma (P_{rad}) and plasma current (I_p), (f) line-averaged density (n_e) and deuterium GP pulses.

pression ratio of neutral particle pressures continuously rise. The lowest electron temperature at inner target is below 3.0 eV. The maximum density is 3.4×10^{19} m^{-3} near $t = 700$ ms, which is lower than the Greenwald density limit $n_G = 4.0 \times 10^{19}$ m^{-3}.

A CDP discharge is obtained by the SMBI at midplane, as shown in Fig. 3. The radiating power fraction is 30–50% and D_α emission in divertor continuously drops. The electron temperatures and pressures at two target plates, radiation power in divertor and the gas compression ratio R_{p0} continuously drop during the detachment, while the radiation power in main plasma clearly increases. The electron temperatures at the targets are below 2.0 eV and the compression ratio $R_{p0} > 10$. The maximum density is 4.6×10^{19} m^{-3} at $t = 850$ ms following current ramping down. No clear high-recycling regime is observed before the detachment, which is consistent with the theoretical prediction [6].

Moreover, it is more difficult to obtain the partial detachment if the Grad-B drift is away from X-point. In a reverse Bt discharge, the electron temperature at inner target is higher than it is at the outer target. The temperature asymmetry deceases with the density rising, as shown in Fig. 4. The lowest temperature at two targets is over 5 eV when $n_e = 2.9 \times 10^{19}$ m^{-3} and $R_{p0} < 8$, suggesting worse plasma performance than the Grad-B drift toward the X-point. On JET [10], the nearly balanced temperatures in inner and outer divertor have been observed when the Grad-B drift is away from X-point. This results in larger density detachment in inner divertor. But despite this Te symmetry, the inner leg detaches earlier than the outer one.

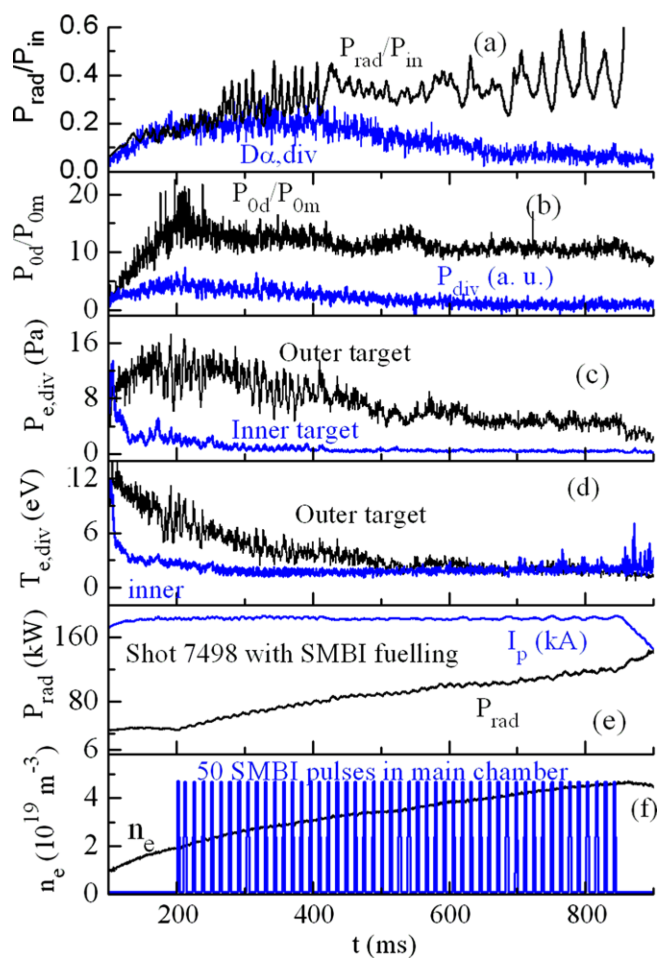

Fig. 3. A CDP discharge with SMBI fuelling at midplane. The curves (a)–(f) are the same as Fig. 2 except 50 SMBI pulses in (f).

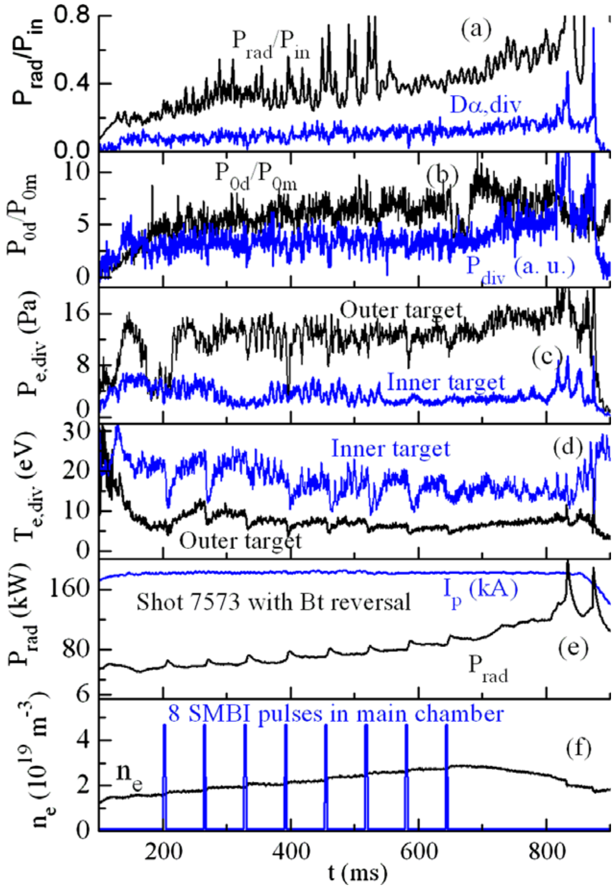

Fig. 4. A attached discharge of Bt reversal with SMBI fuelling in main plasma. The curves (a)–(f) are the same as Fig. 2 except 8 SMBI pulses in (f).

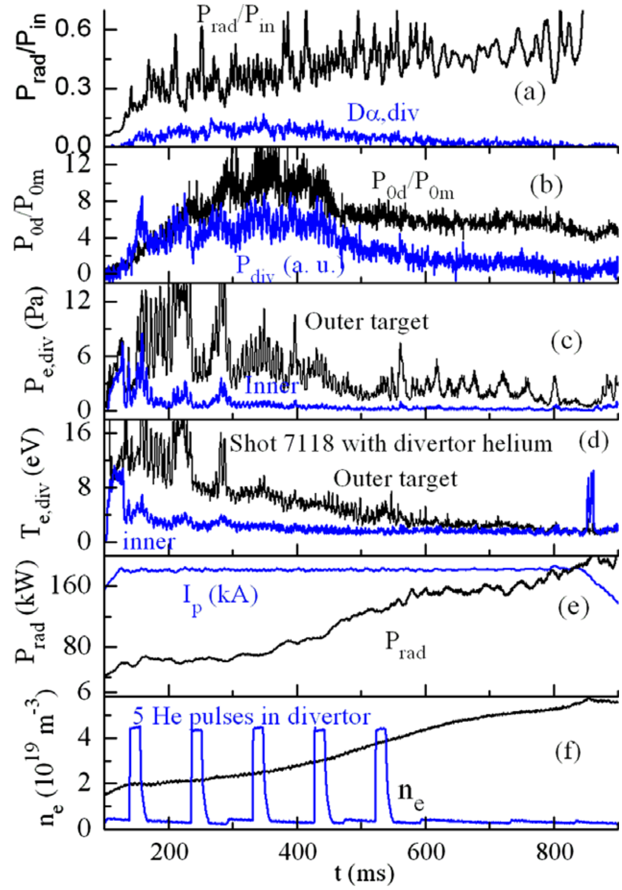

Fig. 5. A CDP discharge with helium puffing in divertor. The curves (a)–(f) are the same as Fig. 2 except 5 divertor helium pulses in (f).

The CDP discharges have also been attained by the deuterium GP and noble gas injection in divertor. The electron temperatures at inner and outer targets are below 2.0 eV. Fig. 5 illustrates a CDP discharge fueled by 5 helium pulses in divertor. Electron temperatures and pressures at target plates, radiation power in divertor and the compression ratio obviously drop during the detachment, while the radiation power in main plasma significantly rises. The electron temperatures at the targets are below 2.0 eV. The maximum density is $5.6 \times 10^{19}\ \mathrm{m}^{-3}$ at $t = 850$ ms before current ramping down and the compression ratio $R_{p0} < 6$ for so high density discharge.

The CDP discharge is also achieved by a neon pulse injected into divertor with very low plasma density, as shown in Fig. 6. The radiating power fraction in main plasma can approach 100% and D_α emission in divertor is extremely low after the neon injection. Electron temperatures and pressures at target plates, radiation power in divertor and the compression ratio abruptly drop during the detachment, while the radiation power in main plasma increases dramatically. The lowest temperature is below 3 eV at inner target, and the maximum density is only $1.8 \times 10^{19}\ \mathrm{m}^{-3}$. The compression ratio is decreased to ~7 from ~20. In addition, the argon gas injection in divertor easily leads to discharge disruption following X-point MARFE formation due to low plasma temperature and high radiating power fraction, which is going to further study in higher temperature and lower radiation fraction plasma. Therefore, the noble gas injection is an effective way to obtain the completely detached plasma.

The estimated decay lengths of power density and electron temperature in linear regime using 'two-point' model in divertor physics [7] are about 0.3 cm and 1.1 cm near the LCFS at mid-plane, respectively. They are extended to ~0.6 cm and ~2.2 cm at the divertor targets due to the expansion of magnetic flux surface and target plate tilting. The temperature decay length is larger than the spatial resolution of flush probes at target plates (1 cm). The movable probe array is used to measure the temperature and pressure profiles in divertor through shot by shot because of higher spatial resolution. Typical profiles with the SMBI fuelling are manifested in Fig. 7. The peak electron temperature and pressure decrease a factor of 8.2 and 8.9 after the SMBI. The measured decay lengths of power density and electron temperature in divertor increase to ~1.6 cm and ~2.7 cm after the SMBI from ~0.9 cm and ~2.2 cm before the SMBI, respectively. These results are in agreement with theoretic prediction [6]. Moreover, the decay length of power density estimated by the IR camera in divertor is higher than that by movable probes. In addition, the electron heat flux, pressure and particle flux in divertor decrease a factor of 75, 34 and 11 after the helium fueling in divertor. These results are consistent with those in Fig. 5 as well. Therefore, the detached discharge can dramatically reduce the heat flux to divertor plate.

4. Summary and discussion

The CDP discharges have been attained using the SMBI at mid-plane, deuterium, helium and neon injections in divertor. Radiation power in divertor gradually drops during the complete detachment because main ionization processes can take place in more upstream region. It is difficult to precisely determine the decay lengths of electron temperature, density and pressure at divertor targets during the detachment because electron temperatures at

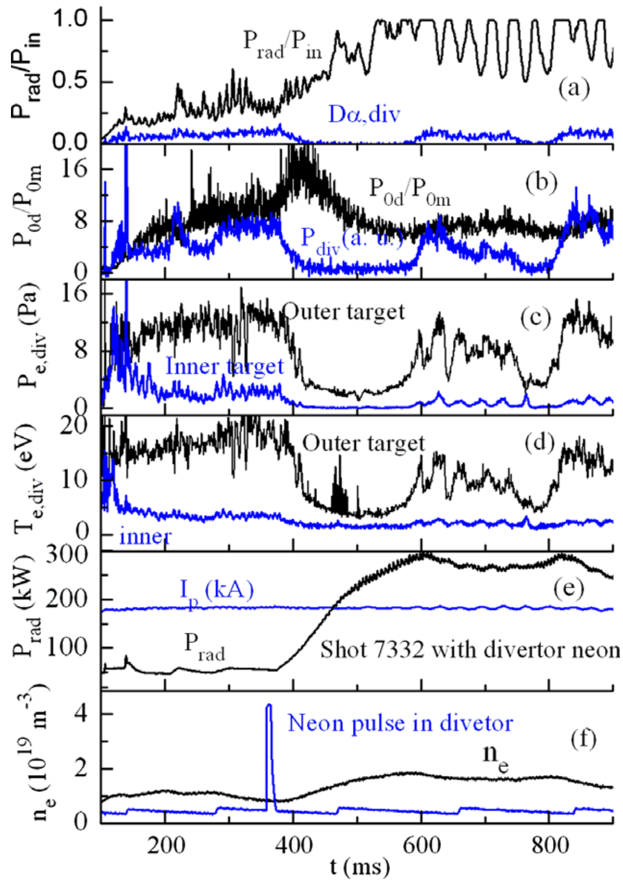

Fig. 6. A CDP discharge with a neon pulse in divertor. The curves (a)–(f) are the same as Fig. 2 except a divertor neon pulse in (f).

the strike points are lower than the around points and bad spatial resolution is at target plates. In addition, the partial detachment is first observed at inner target even if plasma density is very low, i.e., the linear regime in the other tokamaks, which is caused by its specific geometry with narrow and transparent divertor fans. The electron temperature at inner target is higher than it is at outer one when the drift of magnetic field gradient is away from X-point. No clear high-recycling regime is observed in HL-2A before plasma detachment. These experimental results are consistent with simulation results using SOLPS5.0 code [6], especially the detachment of low density discharge.

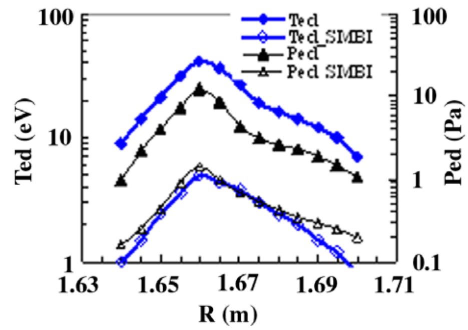

Fig. 7. Electron temperature and pressure profiles versus major radius. The solid, open diamonds and triangles are the electron temperature and pressure profiles in divertor before or after the SMBI, respectively.

Acknowledgment

This work was supported in part by the National Science Foundation of China under the Grant Nos. 10675041 and 10775044.

References

[1] A. Loarte et al., Nucl. Fusion 47 (2007) S203.
[2] H. Takenaga et al., Nucl. Fusion 45 (2005) 1618.
[3] A. Loarte et al., Nucl. Fusion 38 (1998) 331.
[4] T.W. Petrie et al., J. Nucl. Mater. 363–365 (2007) 416.
[5] A. Kallenbach et al., Plasma Phys. Control. Fusion 38 (1996) 2097.
[6] Y.D. Pan, R. Schneider, J. Nucl. Mater. 363–365 (2007) 407.
[7] C.S. Pitcher, P.C. Stangeby, Plasma Phys. Control. Fusion 39 (1997) 779.
[8] Q.W. Yang et al., Nucl. Fusion 47 (2007) S635.
[9] W.Y. Hong et al., Chinese Phys. 15 (2006) 556.
[10] A. Huber et al., J. Nucl. Mater. 337–339 (2005) 241.